Title: Microbial linkages to soil biogeochemical processes in a poorly drained agricultural ecosystem

Authors: Wenjuan Yu[1], Nathaniel C. Lawrence[1], Thanwalee Sooksa-nguan[2], Schuyler D. Smith[2,3], Carlos Tenesaca[1], Adina Chuang Howe[2,3]*, Steven J. Hall[1]*

[1]Department of Ecology, Evolution, and Organismal Biology, Iowa State University, Ames, Iowa, USA

[2]Department of Agricultural and Biosystems Engineering, Iowa State University, Ames, Iowa, USA

[3]Bioinformatics and Computational Biology Program, Iowa State University, Ames, Iowa, USA

*co-corresponding authors: adina@iastate.edu, stevenjh@iastate.edu

Abstract

Soil microorganisms mediate biogeochemical processes, but how microbial community composition influences these processes remains contested. We combined monthly sequencing of soil 16S rRNA genes and intensive measurements of nitrogen (N), carbon (C), and iron (Fe) cycling along a topographic gradient in a poorly drained intensive agricultural ecosystem (corn–soybean rotation) in the midwestern United States. Observed microbial composition changed little over time within and among years despite large differences in weather and crop type. Yet, microbial composition varied greatly with topographic location and correlated strongly with moisture, soil organic carbon (SOC), and especially pH. Microbial families, genera, and/or amplicon sequence variants often correlated significantly with measured biogeochemical processes or pools, yet different taxa within the same phylogenetic groups often responded in opposite ways, indicating a lack of ecological coherence among close relatives. Dominant phyla were generally similar across the topographic gradient but specific members showed consistent tradeoffs among locations. Ammonia oxidizing archaea and bacteria sequences varied oppositely with pH across the gradient, but their combined relative abundances remained similar, as did potential nitrification rates. Nitrospira sequences correlated positively with nitrous oxide (N_2O) fluxes, suggesting a direct or indirect contribution of nitrification (or possibly comammox) to N_2O production. We also found significant linkages between taxonomic groups and redox-sensitive Fe pools, indicating a role for redox variation in structuring microbial communities. Several globally dominant bacteria identified previously correlated significantly with measured biogeochemical variables, providing insights into their possible functional roles. Overall, microbial composition provided a coarse measure of several key biogeochemical functions and implicated taxa that possibly mediate these processes in a widespread agroecosystem of North America.

Keywords: 16S rRNA; iron; nitrification; nitrous oxide; redox; soil health; soil microbial community; soil respiration.

1. Introduction

Microbes mediate soil biogeochemical processes, but whether the composition of the microbial community markedly influences process rates remains contested (E. K. Hall et al., 2018). Furthermore, the ecological roles of many taxa (e.g. amplicon sequence variants, ASVs) remain poorly understood and difficult to characterize (Prosser, 2015). The increasing availability of 16S rRNA gene sequence (hereafter, 16S DNA) data provides a key opportunity for enhancing our understanding of whether and how soil processes might be linked to community composition, and further, for identifying the potential functional roles that globally ubiquitous microbes may play in ecosystems (Delgado-Baquerizo et al., 2018). Here, we evaluated spatiotemporal patterns in microbial community composition and their links to biogeochemical processes by combining frequent 16S DNA sampling with intensive trace gas and soil chemical measurements in an intensive agricultural ecosystem that spanned a broad gradient of soil properties.

Advancing our understanding of microbial linkages to biogeochemical processes is particularly important in soils from intensive agricultural ecosystems, which cause disproportionate environmental impacts and where biophysical variables that influence microbial composition often vary tremendously within individual fields. The Midwestern United States Corn Belt receives the highest inputs of reactive nitrogen (N) of any North American region (Cao et al., 2018), a substantial fraction of which is lost via nitrate leaching or as the greenhouse gas nitrous oxide (N_2O) emission following microbial nitrification and denitrification (Griffis et al., 2017; Jones et al., 2018). Much of this region is characterized by poorly drained soils on undulating post-glacial topography, which must be drained with

subsurface “tiles” to enable cultivation. Even where drainage infrastructure is present, low-lying topographic depressions within individual fields (former “prairie pothole” wetlands) may pond water for periods of days to weeks in most years while upslope soils remain non-flooded (Martin et al., 2019). In addition to large differences in moisture, soil pH may vary by several units across hydric depressions and adjacent upslope areas (tens of meters) as a consequence of carbonate dissolution and precipitation (Logsdon and James, 2014). Soil organic carbon (SOC) stock increases predictably from upslope areas to depressions in this landscape due to erosion (Li et al., 2018). Stark differences in moisture, pH, and SOC created by small elevation changes along topographic gradients provide a unique opportunity to investigate the role of biophysical factors in shaping microbial communities and their biogeochemical processes (Suriyavirun et al., 2019).

Changes in moisture along topographic gradients alter the availability of oxygen (O_2) and redox-sensitive iron (Fe) pools, which may also be linked to variation in microbial composition (Suriyavirun et al., 2019). Iron(III) is an important anaerobic electron acceptor even in nitrate-rich agricultural soils (Huang and Hall, 2017a). Reduced (Fe(II)) and oxidized (Fe(III)) forms of Fe are sensitive to O_2 availability, which varies dynamically with soil moisture. Therefore, extractable Fe(II) serves as a relative metric of anoxia within a given soil sample (Hall et al., 2013). At low-lying locations experiencing more frequent redox fluctuations, larger pools of highly reactive Fe(III) may be formed relative to upslope locations (Suriyavirun et al., 2019). Redox traits provide a fundamental constraint on microbial community composition at global scales (Ramírez-Flandes et al., 2019). Yet, whether and how redox variation structures the composition of soil microbial communities remains understudied in terrestrial ecosystems (Pett-Ridge and Firestone, 2005; Suriyavirun et al., 2019).

The high spatial and temporal variation in moisture and reactive nitrogen inputs

characteristic of Corn Belt agricultural ecosystems also provides an important opportunity to examine links between microbes and soil N-cycling processes such as N mineralization, nitrification, and N_2O production. The abundance and diversity of functional genes encoding enzymes involved in nitrification and denitrification have often been compared with biogeochemical process rates (e.g. N_2O production) or N pools (Domeignoz□Horta et al., 2018; Petersen et al., 2012), but linkages between 16S community composition and process rates remain relatively poorly explored (Pitombo et al., 2016; Suriyavirun et al., 2019). For example, ammonia oxidizing archaea and bacteria (AOA and AOB) both oxidize ammonia to hydroxylamine using ammonia monooxygenase, but whether variation in these groups correlates with changes in nitrification rates or N_2O production is unclear, especially in agricultural systems. In particular, the high temporal variability that characterizes most N-cycling processes in soils (Butterbach-Bahl et al., 2013) creates a challenge for linking pools or fluxes with microbial composition.

Most biogeochemical process rates are seasonally dynamic, but we do not know if these will be recorded by seasonal variations in DNA sequences, and relatively few studies have sampled DNA with sufficient frequency to concretely assess within- or among-year variation. The 16S DNA extracted from soil provides an integrated measure of the taxonomic composition of living, dormant, and recently deceased microbes (Carini et al., 2016). Agricultural soil microbial communities may vary seasonally along with temperature and moisture (Bainard et al., 2016; Lauber et al., 2013). Apart from abiotic factors, crop type is also a primary driver of changes in soil microbial communities, through variation in quality and quantity of litter inputs and root exudates (Hsiao et al., 2019). Yet despite the widespread use of crop rotations, few studies have focused on interannual changes in soil microbes within rotation systems and both major (Hsiao et al., 2019) or minor (Smith et al., 2016) effects of crops have been reported. Most studies of microbial change in agricultural soils

112 focused on a single year (Lauber et al., 2013), or had sparse resolution among years (Smith et
113 al., 2016; Upton et al., 2019), such that potential temporal variation in microbial communities
114 could not be assessed along with other agroecological and biogeochemical processes in crop
115 rotations.

116 Finally, when assessing potential linkages among microbial community composition and
117 biogeochemical processes, we are confronted with the question of taxonomic scale: are
118 closely related taxa within broader taxonomic groups ecologically coherent (sensu Philippot
119 et al., 2010)? On one hand, subpopulations of the same species might carry out different
120 functions as indicated by genomic studies (Kashtan et al., 2014; Rasko et al., 2008). On the
121 other hand, functional redundancy of lower taxonomic groups (e.g. ASV) and life-history
122 coherence at high bacterial taxonomic ranks (e.g. phylum) have also been widely highlighted
123 (García-García et al., 2019; Philippot et al., 2010). Examination of relationships among
124 biogeochemical processes and particular ASVs and broader taxonomic groups would reveal if
125 these relationships were consistent among closely related taxa.

126 Here, we investigated spatio-temporal variation in soil microbial community
127 composition, the dominant drivers of the variation, and linkages with biogeochemical
128 processes by combining 16S rRNA gene analyses with soil trace gas fluxes and chemical
129 extractions. We collected mineral soils along a topographic gradient in a corn (*Zea mays*) -
130 soybean (*Glycine max*) rotation system in central Iowa, U.S.A., over two years on an
131 approximately monthly basis when soils were not frozen. Meanwhile, we measured N_2O and
132 carbon dioxide (CO_2) fluxes at high frequency (every 4 h) along the transect, leveraging a
133 novel automated gas measurement system (Lawrence and Hall, 2020). Using measurements
134 of greenhouse gas fluxes and soil chemical extractions, we explored associations among
135 microbial community composition and several N- and C-cycling processes and
136 redox-sensitive Fe pools, both at higher (family and genus) and low (ASV) taxonomic levels.

We addressed the following questions: 1) Does microbial community composition vary along the field-scale topographic gradient and with time, and what are the dominant drivers of the variation? 2) are microbial taxonomic groups and ASVs linked to measurements of C, N, and Fe cycling?

2. Materials and methods

2.1. Study site and field sampling

We established eight sampling locations at intervals of approximately 17 m along a topographic gradient spanning a depression to an adjacent upslope area in an agricultural field in central Iowa, USA (41.98° N, 93.69° W; Fig. 1a). The transect spanned 120 m with an elevation change of 2.25 m and included very poorly to moderately poorly drained Mollisols in the Okoboji, Canisteo, and Nicollet soil series in the U.S. Department of Agriculture classification. Elevation of each sampling location relative to the bottom of the depression was assessed using a digital elevation model (Gelder, 2015). Occasional flooding occurred in the lower half of the transect despite the presence of subsurface drainage tile and surface tile inlets (Martin et al., 2019). Flooding events caused partial crop mortality in locations 1–2 in 2017 and complete crop mortality in locations 1–4 in 2018 (location 1 is lowest and 8 is highest, respectively). Corn (*Zea mays*, planted 2017) and soybean (*Glycine max*, planted 2018) have been cultivated in annual rotation at this site for several decades. Agricultural management was typical for the region and included urea-ammonium-nitrate fertilizer applied in April and June 2017 for a total of 179 kg N ha^{-1} and tillage in November 2017. Although our measurements were limited to a single transect and field due to the intensive nature of our sampling, corn-soybean rotations on poorly drained soils are a major land-cover type of the Midwestern U.S. (Martin et al., 2019).

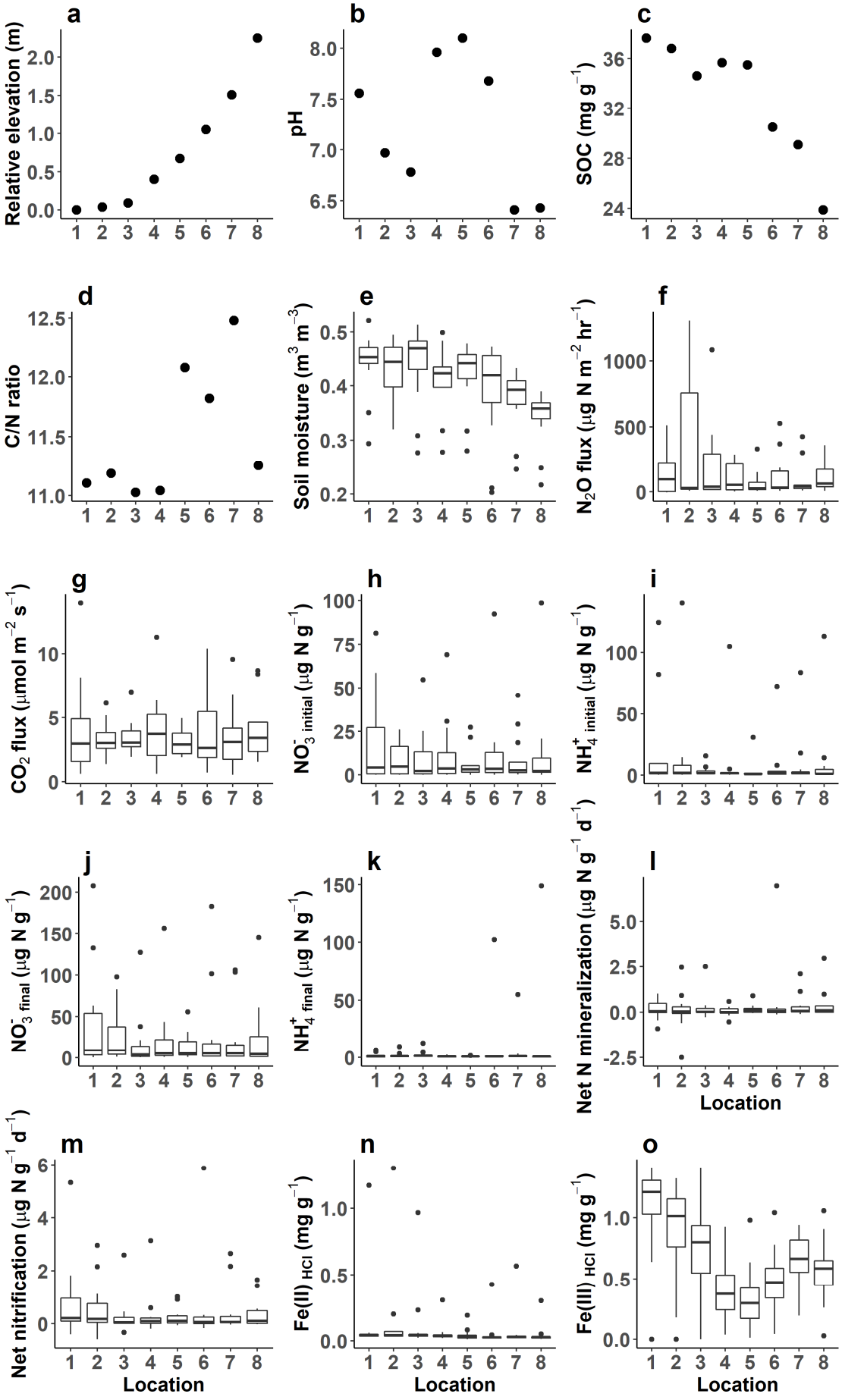
a
Relative elevation (m)
b
pH
c
SOC (mg g^{-1})
d
C/N ratio
e
Soil moisture (m^3 m^{-3})
f
N_2O flux (μg N m^{-2} hr^{-1})
g
CO_2 flux (μmol m^{-2} s^{-1})
h
NO_3^- initial (μg N g^{-1})
i
NH_4^+ initial (μg N g^{-1})
j
NO_3^- final (μg N g^{-1})
k
NH_4^+ final (μg N g^{-1})
l
Net N mineralization (μg N g^{-1} d^{-1})
m
Net nitrification (μg N g^{-1} d^{-1})
n
Fe(II) HCl (mg g^{-1})
o
Fe(III) HCl (mg g^{-1})
Location

160

Fig. 1. Environmental variables across eight sampling locations distributed at intervals of approximately 17 m along a topographic gradient in an agricultural field in central Iowa, USA. The transect spans 120 m length and 2.25 m elevation. Location 1 is lowest and location 8 is highest. $NO_3^-{}_{initial}$ and $NO_3^-{}_{final}$ represent initial and final concentrations of nitrate before and after incubation, respectively; $NH_4^+{}_{initial}$ and $NH_4^+{}_{final}$ represent initial and final concentrations of ammonium before and after incubation, respectively.

We collected soils 12 times during the study period: April 2017, May 2017, June 2017, September 2017, March 2018, April 2018, May 2018, June 2018, July 2018, August 2018, September 2018, and October 2018. Soils were collected in a single morning during the latter half of each month. For each sampling, mineral soil cores were collected at 0–10 cm depth with a stainless-steel soil corer (7.3 cm diameter) from three places at each location along the transect: immediately adjacent to the crop row, a median position between two rows, and an intermediate position. The row spacing (76 cm) left approximately 17 cm between core midpoints. Soils were transported in a cooler to our laboratory immediately and soil processing was completed within 6 h. Visible plant material and stones were removed by hand. Approximately 10 g was subsampled from each soil and stored at -80°C for subsequent DNA extraction.

2.2. Laboratory soil property analyses and field measurements

Soils collected in May 2018 were air-dried and sieved (2 mm) for analysis of selected soil properties. Soil pH was measured with a soil-to-water mass:volume ratio of 1:1. Soil bulk C and N concentrations were analyzed by a Vario Micro Cube elemental analyzer (Elementar, Langenselbold Germany). We calculated carbonate content by measuring CO_2 produced from HCl-treated soils (Ye and Hall, 2020), and SOC was calculated as the difference between bulk C and carbonate C concentrations.

Soil properties related to N- and Fe-cycling processes were analyzed using field-moist samples immediately following each collection date described above. Nitrate (NO_3^-) and ammonium (NH_4^+) were extracted by 2M potassium chloride (1:5 ratio of dry mass equivalent to solution) and their N concentrations were analyzed by colorimetric microplate assays (Doane and Horwáth, 2003; Weatherburn, 1967) and expressed as $NO_3^-{}_{initial}$ and $NH_4^+{}_{initial}$, respectively. To calculate potential N mineralization, subsamples were placed in open vials in a humidified headspace and incubated at field moisture and lab temperature (~23°C) for 28 d. After incubation, these soils were extracted and analyzed using the same methods described above to quantify $NO_3^-{}_{final}$ and $NH_4^+{}_{final}$, respectively. Net N mineralization was calculated as the change in the sum of NO_3^--N and NH_4^+-N pools, and net nitrification was calculated as the change in NO_3^--N pool over 28 d. To measure Fe(II), which readily oxidizes to Fe(III) in the presence of O_2, soil samples were briefly homogenized in a plastic bag within seconds of field collection and a subsample was immediately added to a pre-weighed centrifuge tube with 0.5 M HCl (target ratio of 1:15 soil to acid) to prevent oxidation of Fe(II), hereafter denoted $Fe(II)_{HCl}$ (Huang and Hall, 2017b). Once in the laboratory, samples were vortexed for 1 min, extracted for 1 h on a rotary shaker, and centrifuged for 10 min at 10,000 g. The supernatant solution was carefully decanted to a clean container and $Fe(II)_{HCl}$ and $Fe(III)_{HCl}$ were analyzed using a ferrozine method optimized for soil extractions (Huang and Hall, 2017b).

In the field, we measured fluxes of N_2O and CO_2, along with soil moisture and temperature, at each location during the study period. During periods when living plants were present (May–October), CO_2 flux includes both heterotrophic and autotrophic respiration. Soil moisture (~0–20 cm depth) was recorded in all locations every 10 min using CS616 moisture probes installed at a 45º angle relative to the soil surface (Campbell Scientific, Logan UT). Soil temperature was recorded for several locations every 10 min using CS107

211 sensors (Campbell Scientific, Logan UT) at 10 cm depth. Soil N_2O and CO_2 fluxes were
212 measured once every 4 h by an automated flux chamber at each location (a second chamber
213 was added to each location in July 2018 and the flux data afterwards was an average of the
214 two chambers per location). The chamber system was described in detail by Lawrence and
215 Hall (2020). To match with microbial data, the values in the 15 d prior to soil sampling were
216 averaged for each of the four variables. This timescale was chosen given the fact that
217 microorganisms can turn over on timescales of weeks to months (Spohn et al., 2016). There
218 were some data gaps caused by agricultural management and/or instrument failure. Two
219 missing moisture values for one sampling time were filled by the averages of their respective
220 adjacent locations. Missing temperature values in other locations were filled by the averages
221 of the recorded locations. Missing flux data were not gap-filled.

222 2.3. DNA extraction and 16S rRNA gene amplicon sequencing

223 We extracted DNA from 285 samples (12 months × 8 locations × 3 cores; three samples
224 from September 2017 could not be analyzed due to technical constraints). Subsamples of 250
225 mg were extracted using the PowerSoil 96 Well DNA Isolation Kit (Qiagen, USA).
226 Concentrations of DNA were measured using a DNA Quantification Kit Q33120
227 (ThermoFisher, USA) to enable subsampling of a standard DNA mass for sequencing.
228 Samples were diluted to 10 ng DNA μL^{-1} prior to sequencing; samples with concentration <
229 10 ng DNA μL^{-1} were submitted directly. The V4 region of bacterial and archaeal 16S rRNA
230 genes (254 bp in most species) was amplified using the 515F
231 (GTGYCAGCMGCCGCGGTAA) / 806R (GGACTACNVGGGTWTCTAAT) primers.
232 Before sequencing, a library was prepared following the EMP 16S Illumina Amplicon
233 protocol (Caporaso, 2018). Sequencing of archaeal and bacterial amplicons was performed on
234 an Illumina Miseq sequencer with Miseq Reagent Kit V2 (Illumina, USA) at Argonne
235 National Laboratory, producing 2 × 150-bp reads. Sequences were deposited in the NCBI

236 Sequence Read Archive under BioProject accession number PRJNA678372.

237 *2.4. Bioinformatics*

238 We used the Divisive Amplicon Denoising Algorithm 2 (DADA2) pipeline (Callahan et
239 al., 2016) to process the sequencing data in R statistical software version 3.6.1 (R Core Team,
240 2019). Three samples were not included due to a small number of reads (≤ 32 sequences).
241 Most functions were run using parameters suggested by the DADA2 pipeline tutorial (version
242 1.16). During filtering, bases after 145 in both forward and backward reads were truncated
243 after inspecting read quality. Merging each pair of truncated reads (145 bp) gave sequences of
244 approximately 254 bp, with 36 bp overlapping. Sequences > 256 bp or < 250 bp might result
245 from non-specific priming and were removed. In the chimera removing step, the "pooled"
246 method was applied as it produced more reasonable chimera detection results compared with
247 the "consensus" method. The end product included an ASV table recording the number of
248 times each exact ASV was observed in each sample, along with a taxa table recording
249 taxonomy assigned to the ASVs from domain to genus levels, using the Ribosomal Database
250 Project classifier algorithm and the Silva database version 132.

251 Next, we trimmed the ASV and taxa tables using the "phyloseq" package version 1.30.0
252 (McMurdie and Holmes, 2013) in R. Any ASVs from mitochondria, chloroplast, or
253 eukaryotes were excluded from further analyses. Samples containing < 200 ASVs were
254 removed (15 samples) and ASVs that did not have at least five sequences in at least two
255 samples were also removed. Removal of rare taxa decreases noise in subsequent statistical
256 analyses because their presence may reflect stochastic factors more than underlying biology;
257 our approach resulted in slightly more taxa retained than in the example method for the
258 phyloseq package. Before trimming, there were 15009 total ASVs and 3597687 total
259 sequences across 282 samples; afterwards, there were 5633 total ASVs and 3477159 total
260 sequences across 267 samples. There were 209 to 603 ASVs (mean = 433) and 5063 to 20904

sequences per sample (mean = 13023). Rarefaction curves showed that sequencing depths were adequate for all samples (data not shown). There were no apparent biases against location, core, or sampling month of the 18 omitted samples, although they were all collected in 2018.

2.5. Statistical analyses

All statistical analyses were performed in R software. Six environmental variables were log10 transformed to reduce skewness: N_2O flux, $NO_3^-{}_{initial}$, $NH_4^+{}_{initial}$, $NO_3^-{}_{final}$, $NH_4^+{}_{final}$, and $Fe(II)_{HCl}$. Three-way ANOVA analyses without interaction followed by Tukey's multiple comparison tests (if needed) were used to test for differences in greenhouse gas fluxes, soil properties, relative abundances of AOA and AOB, and alpha diversity among locations, years (crops), and months. All three factors were fixed effects. Alpha diversity was assessed using chao1, Shannon, and inverse Simpson indices. Redundancy analyses (RDA) based on Bray-Curtis dissimilarities were performed using the "vegan" package (Oksanen et al., 2019) to visualize overall community composition and to identify correlated environmental variables. Seventeen explanatory variables, namely year, month, pH, SOC concentration, C/N ratio, soil temperature, soil moisture, relative elevation, $NO_3^-{}_{initial}$, $NH_4^+{}_{initial}$, $NO_3^-{}_{final}$, $NH_4^+{}_{final}$, net N mineralization, $Fe(II)_{HCl}$, $Fe(III)_{HCl}$, N_2O flux, and CO_2 flux, were used in the RDA analysis. We used single measurements of pH and SOC pooled by location (means of three replicates) because these variables change slowly relative to our microbial sampling interval (i.e., nearby soils showed no management impacts on SOC or pH after 10 y; Ye and Hall, 2020). All other predictor variables were measured along with each microbial sample, thus representing temporal as well as spatial variation. Permutational multivariate analysis of variance (PERMANOVA) based on Bray-Curtis dissimilarities was also performed using the "vegan" package to test effects of the above-mentioned 17 variables on community composition. In RDA and PERMANOVA analyses, we performed model selection by

removing insignificant variables ($P < 0.01$), starting with the variable with the highest *P*-value and F-value, respectively. The DESeq2 package (Love et al., 2014) was used to identify ASVs that differed significantly among topographic locations. To account for constant values of pH and SOC at each location over time, relationships among pH and SOC and dominant phyla and classes were explored by linear mixed model (LMM) analyses with location as a random effect using the "lme4" package (Bates et al., 2015). The associations among soil moisture and these microbial groups were explored by Spearman correlation analyses. The Spearman correlation analyses were also performed to study the relationships among N- and Fe-cycling processes and microbial groups that are reported to be associated with these processes (Esther et al., 2015; Guo et al., 2019; Kuypers et al., 2018; Philippot and Germon, 2005; Weber et al., 2006), as well as individual ASVs within these taxonomic groups, using the "phylosmith" package (Smith, 2019). Nine N- and Fe-cycling variables were included for the correlation analyses: N_2O flux, $NO_3^-{}_{initial}$, $NH_4^+{}_{initial}$, $NO_3^-{}_{final}$, $NH_4^+{}_{final}$, net N mineralization, net nitrification, $Fe(II)_{HCl}$, and $Fe(III)_{HCl}$. The correlation analyses were also utilized to explore relationships of CO_2 flux and the above-mentioned nine biogeochemical variables with ASVs that corresponded with globally dominant bacterial operational taxonomic units (OTUs) identified in a previous study (Delgado-Baquerizo et al., 2018). Bonferroni adjustment was used for ANOVA and correlation/LMM analyses whereby individual P values were multiplied by the number of tests conducted to correct for multiple comparisons using the "p.adjust" R function with the "method" argument set to "bonferroni" (Jafari and Ansari-Pour, 2019). Due to the conservative nature of the Bonferroni adjustment, we defined a significance threshold for the Bonferroni-adjusted *P* values at 0.10.

In a preliminary PERMANOVA analysis, sampling position of each core relative to the crop row was insignificant ($P > 0.05$) and only explained 0.5% of community composition. Therefore, we averaged all environmental and microbial data for the three replicate cores per

location per sampling date for statistical analyses (i.e., 267 total samples were reduced to 95 mean samples). We used 74–87 and 94 mean samples when including N-cycling and Fe-cycling processes, respectively, due to missing values in the related soil properties. Alpha diversity indices were calculated on a per-sample basis prior to averaging by sampling location/date. Microbial analyses were conducted using relative abundances of ASVs or higher taxonomic groups, except for DESeq2 and alpha diversity analyses, which used absolute abundances of ASVs.

3. Results

3.1. Soil properties and greenhouse gas fluxes

Soils across the topographic gradient differed strongly in pH (6.4–8.1) and SOC (24–38 mg g^{-1}), with smaller variation in soil C:N (11.0–12.5; Fig. 1; Table S1). Despite large temporal variation, location-level mean values also significantly differed in soil moisture (33.7–43.9%), $Fe(III)_{HCl}$ (0.34–1.05 mg g^{-1}), and $Fe(II)_{HCl}$ (0.05–0.16 mg g^{-1}). Soil pH was highest (7.7–8.1) in the intermediate locations (0.40–1.05 m relative elevation) and lowest (6.4) in the upslope locations (1.51–2.25 m relative elevation). SOC concentration decreased from the lowest to highest location (37.7 mg g^{-1} to 23.9 mg g^{-1}), as did location-level mean soil moisture (43.9 ± 1.8% to 33.7 ± 1.6%). Location-level mean $Fe(III)_{HCl}$ was higher in the bottom of the depression (0.00–0.09 m relative elevation; 0.75 ± 0.11 to 1.05 ± 0.12 mg g^{-1}) compared with other locations (0.34 ± 0.08 to 0.65 ± 0.07 mg g^{-1}). However, the dynamic soil properties measured here differed more over time (months and years) than among topographic locations. For example, mean $NO_{3\,final}^{-}$ was higher in 2017 (66.02 ± 10.09 μg N g^{-1}) than in 2018 (4.22 ± 0.43 μg N g^{-1}), as expected given that N fertilizer was applied during the corn phase. Monthly mean $Fe(II)_{HCl}$ was significantly higher in July (0.65 ± 0.36 mg g^{-1}) than in other months (0.03 ± 0.004 to 0.05 ± 0.004 mg g^{-1}). Fluxes of N_2O (overall range:

-5.72–1315.47 μg N m^{-2} hr^{-1}) and CO_2 (overall range: 0.54–13.96 μmol m^{-2} s^{-1}) also varied greatly over time (Fig. 1).

3.2. Drivers of soil microbial community composition

Microbial communities did not group strongly by year or month in RDA analysis based on Bray-Curtis dissimilarities (Fig. S1). However, RDA revealed a clear separation of microbial communities by topographic location, with locations 1, 2, and 3 (0.00–0.09 m relative elevation), locations 4 and 5 (0.40–0.67 m relative elevation), location 6 (1.05 m relative elevation), and locations 7 and 8 (1.51–2.25 m relative elevation) forming separate clusters (Fig. 2). The first two axes (PC1 and PC2) explained 85.1% of the variation of overall community composition and had significant relationships ($P < 0.01$) with six environmental variables (pH, relative elevation, SOC, C/N ratio, $Fe(III)_{HCl}$, and moisture), which explained 52.1% of the composition variation (Fig. 2). Nine significant variables ($P < 0.01$) explained 64.1% of the variation in microbial community composition as shown by PERMANOVA analysis (Table S2). Soil pH explained the most variation (28.3%), followed by relative elevation (12.5%), month (6.6%), soil moisture (6.4%), SOC concentration (3.0%), C/N ratio (2.3%), soil temperature (1.7%), $Fe(III)_{HCl}$ (1.7%), and year (1.6%). The other biogeochemical variables (e.g. N_2O and CO_2 fluxes) were not significantly related to community composition in the RDA. Microbial ASV richness (Chao1 index) and diversity (Shannon index) did not significantly differ between years or among months or locations (Fig. S2). Microbial evenness (inverse Simpson index) significantly differed among months and locations ($P < 0.05$); it was generally higher from July to October compared with March to June and was lower at location seven than the others.

Fig. 2. Redundancy analysis based on Bray-Curtis distance demonstrating differences in overall microbial community composition among topographic locations (1 is lowest, 8 is highest), which clustered in four groups. Only significant ($P < 0.01$) explanatory variables are shown in blue arrows. Moisture and Fe(III)HCl were measured along with each microbial community sample to capture temporal variation; the other variables were measured at a single timepoint.

We further evaluated the relationships among pH, moisture, SOC concentration, and dominant phyla and classes (Fig. 3). Among the significant relationships (Bonferroni-adjusted $P < 0.10$), pH had negative relationships with relative abundances of *Verrucomicrobia* (standardized slope = -0.77) and *Acidobacteria Acidobacteriia* (-0.73) and positive relationships with *Thaumarchaeota* (0.67), *Actinobacteria* (0.50) and *Acidobacteria* subgroup 6 (0.40). Soil moisture had positive relationships with relative abundances of *Acidobacteria* (r = 0.42), *Chloroflexi* (r = 0.32), *Gemmatimonadetes* (r = 0.44), *Deltaproteobacteria* (r = 0.48), and *Acidobacteria* subgroup 4 (r = 0.38) and negative relationships with *Bacteroidetes* (r = -0.39) and *Verrucomicrobia* (r = -0.44). SOC had negative relationships with

374 *Verrucomicrobia* (-0.76) and *Bacteroidetes* (-0.32) and a positive relationship with
375 *Chloroflexi* (0.62).

376
377 **Fig. 3**. The relationships between relative abundances of dominant phyla and classes and pH,
378 moisture, and SOC concentration assessed using linear mixed models (for pH and SOC) and
379 Spearman correlations (for moisture). A circle is present if Bonferroni-adjusted *P* is < 0.1,
380 with circle size indicating strength of the relationship. The color indicates the direction of
381 relationship (blue is positive, red is negative) and the number represents the standardized
382 slope or correlation coefficient. Dominant phyla are arranged in order of decreasing relative
383 abundance, and all three classes in *Proteobacteria* and three dominant classes in
384 *Acidobacteria* comprising 88% of total sequences in the phylum are also included.

385

386 *3.3. Relationships among microbial groups and biogeochemical processes*

387 We identified several microbial groups that were significantly related to measurements
388 of N-cycling processes (Fig. 4). Relative abundance of *Cytophagaceae* was positively
389 correlated with $NO_3^-{}_{initial}$, $NH_4^+{}_{initial}$, and $NO_3^-{}_{final}$. *Nitrospiraceae* was positively related to
390 N_2O fluxes. *Ferruginibacter* was positively related with $NO_3^-{}_{initial}$ and $NH_4^+{}_{initial}$. *Litorilinea*
391 was positively related with $NH_4^+{}_{initial}$. Individual ASVs within some groups were consistently
392 correlated with metrics of N transformation. For example, four ASVs within the
393 *Ferruginibacter* genus all had a significantly positive correlation with $NH_4^+{}_{initial}$

(Bonferroni-adjusted $P < 0.10$), leading to a significantly positive correlation between the genus and $NH_4^+{}_{initial}$. Meanwhile, ASVs within some groups showed different relationships to N cycling. For example, two ASVs within the *Nitrospiraceae* family showed opposite relationships with $NH_4^+{}_{initial}$, leading to a lack of significant correlation between the family and $NH_4^+{}_{initial}$. Relative abundances of Fe-reducing *Anaeromyxobacter* and Fe-oxidizing *Rhodomicrobium* were positively correlated with $Fe(II)_{HCl}$; Fe-reducing *Bacillus* and Fe-oxidizing *Thermomonas* were positively and negatively correlated with $Fe(III)_{HCl}$, respectively (Fig. 5). Some ASVs within broader taxonomic groups (e.g. *Anaeromyxobacter)* showed consistent responses to $Fe(II)_{HCl}$, while some (e.g. ASVs within *Geobacter*) showed opposing responses (i.e., both positive and negative) to $Fe(III)_{HCl}$.

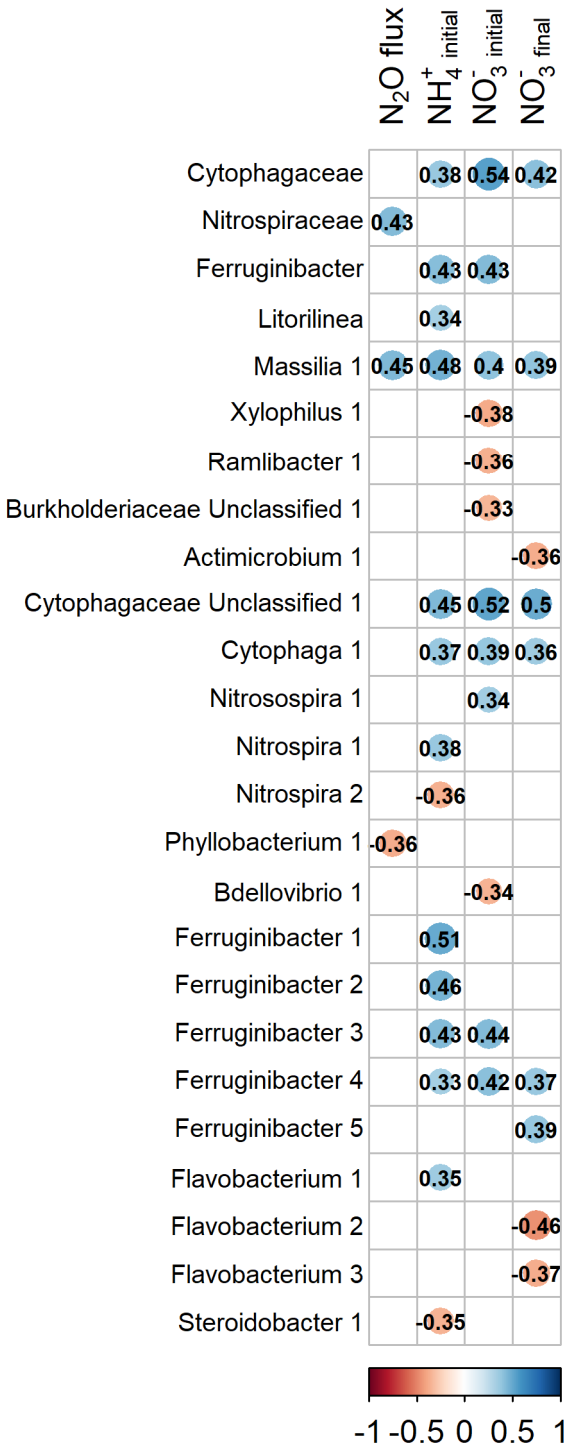

404

405 **Fig. 4**. Significant Spearman correlations between N-cycling processes and relative
406 abundances of microbial groups and ASVs thought to participate in N-cycling. Correlations
407 reflect both spatial and temporal variation, as microbes and biogeochemical variables were

measured in each sample over time. A circle is present if Bonferroni-adjusted *P* is < 0.1, with circle size indicating strength of the relationship (and absence of circle indicating no significant relationship) and number in a circle indicating correlation coefficient. The color indicates the direction of relationship (blue is positive, red is negative). A family or genus followed by a number denotes that a particular ASV within that group exhibited a significant correlation with an N-cycling variable. $NO_3^-{}_{initial}$ and $NO_3^-{}_{final}$ represent initial and final concentrations of nitrate before and after incubation, respectively; $NH_4^+{}_{initial}$ represents initial concentration of ammonium before incubation. Net N mineralization, net nitrification, and final concentration of NH_4^+ were not shown due to very few significant relationships between these processes and microbial groups or ASVs.

418

419 **Fig. 5**. Significant Spearman correlations between Fe-cycling pools and relative abundances
420 of microbial groups and ASVs thought to participate in Fe-cycling. Correlations reflect both
421 spatial and temporal variation, as microbes and biogeochemical variables were measured in
422 each sample over time. A circle is present if Bonferroni-adjusted *P* is < 0.1, with circle size
423 indicating strength of the relationship (and absence of circle indicating no significant
424 relationship) and number in a circle indicating correlation coefficient. The color indicates the
425 direction of relationship (blue is positive, red is negative). A genus followed by a number
426 denotes that a particular ASV within the genus significantly correlated with $Fe(II)_{HCl}$ or

427 $Fe(III)_{HCl}$.

428

429 Beyond the groups and taxa described above, we also found that some of the globally
430 dominant bacterial OTUs identified previously (Delgado-Baquerizo et al., 2018) that were
431 present in our samples showed significant relationships with biogeochemical processes (Table
432 S3). Relative abundances of many of these ASVs correlated with $Fe(III)_{HCl}$, and most
433 belonged to *Chitinophagaceae* (e.g. *Flavisolibacter* and *Segetibacter*) and had positive
434 relationships with $Fe(III)_{HCl}$. Two *Haliangium* ASVs had positive relationships with
435 $Fe(III)_{HCl}$, two *Agromyces* ASVs had negative relationships, and ASVs within *Gaiella*, *67-14*,
436 *Sphingomonas*, and *Chthoniobacter* had mixed relationships with $Fe(III)_{HCl}$. Some ASVs
437 within *Chthoniobacter* and *Haliangium* were also closely related to $Fe(II)_{HCl}$. Several groups
438 had an ASV significantly correlated with multiple N-cycling variables: *Flavisolibacter*
439 (positive), *Pseudarthrobacter* (negative), and *WD2101_soil_group* (positive; Table S3). Two
440 ASVs within *Sphingomonas* were either positively or negatively associated with CO_2 flux.

441 *3.4 Tradeoffs among ASVs and groups*

442 Across all topographic locations, eight dominant prokaryote phyla had > 2% sequence
443 relative abundance (Fig. S3). These included *Proteobacteria* (25.3%), *Acidobacteria* (21.3%),
444 *Bacteroidetes* (16.3%), *Actinobacteria* (9.9%), *Verrucomicrobia* (8.7%), *Chloroflexi* (4.3%),
445 *Gemmatimonadetes* (3.0%), and *Thaumarchaeota* (4.0%). These phyla accounted for 92.9%
446 of total sequences and were dominant in each topographic location, with only minor changes
447 in relative abundances among locations (Fig. S3). Despite the consistency in phylum-level
448 abundance, Deseq2 analysis showed tradeoffs among ASVs within each phylum, i.e., some
449 ASVs within each dominant phylum significantly ($P < 0.01$) increased with relative elevation
450 while others significantly decreased (Fig. 6). Median log2-fold changes of *Bacteroidetes* and
451 *Verrucomicrobia* with relative elevation were positive, while those of other phyla were

452 negative. A tradeoff in relative abundance among sampling locations was also observed
453 between archaeal and bacterial ammonia-oxidizing groups, which together comprised a large
454 mean proportion of sequences at each sampling location (4.6–7.2%; Fig. 7; multiple
455 comparison tests are shown in the figure). Relative abundance of *Nitrososphaeraceae* (AOA)
456 was significantly highest (5.5–5.7%) in locations 4 and 5 and lowest (1.8%) in location 8. In
457 contrast, relative abundance of *Nitrosomonadaceae* (AOB) was lowest (1.5%) in locations 4
458 and 5 and highest in location 8 (2.8%). *Nitrososphaeraceae* had a strong positive relationship
459 with pH (r = 0.67; $P < 0.05$) while *Nitrosomonadaceae* had a negative relationship with pH (r
460 = -0.43; $P < 0.05$).

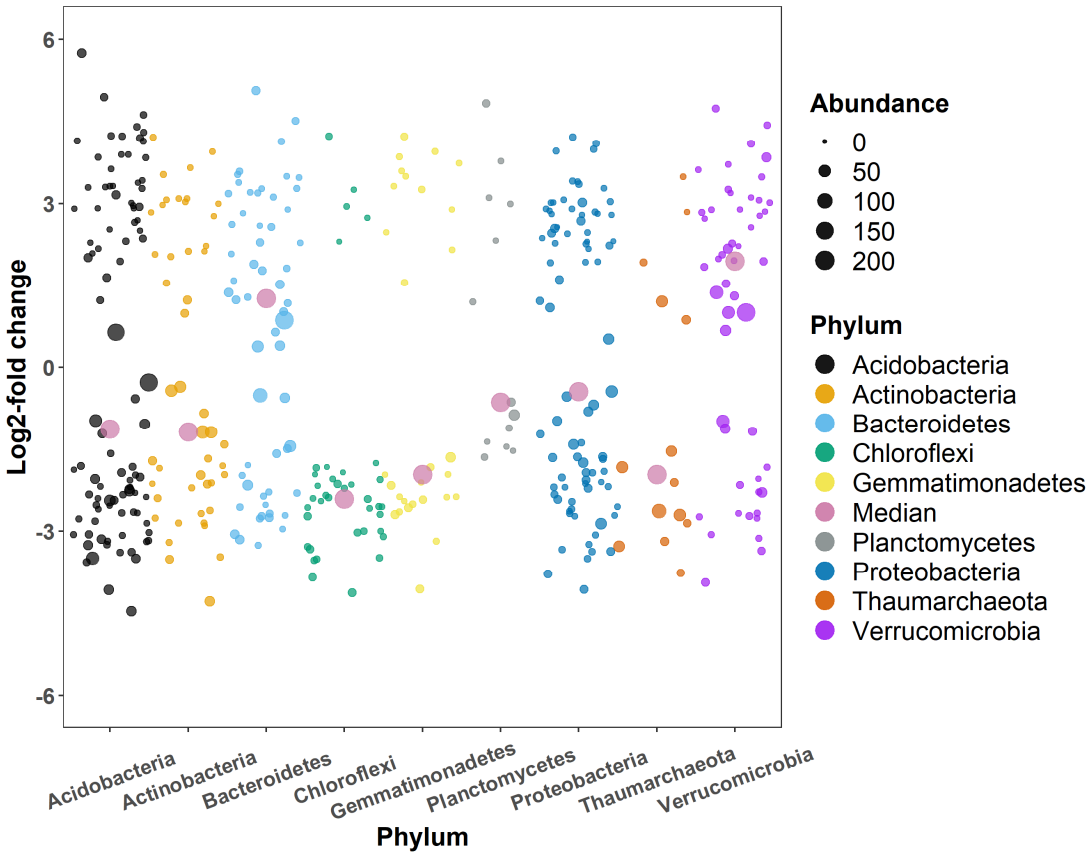

461
462 **Fig. 6.** Log2-fold change in ASV abundance with relative elevation for dominant phyla,
463 assessed using DESeq2 analysis. Each circle represents an ASV that significantly varied with
464 relative elevation (Benjamini and Hochberg-adjusted $P < 0.01$). Circle size indicates the
465 average of the normalized abundances, dividing by size factors, taken over all samples. A

466 pink circle represents the median response of log2-fold change to relative elevation for a
467 phylum.

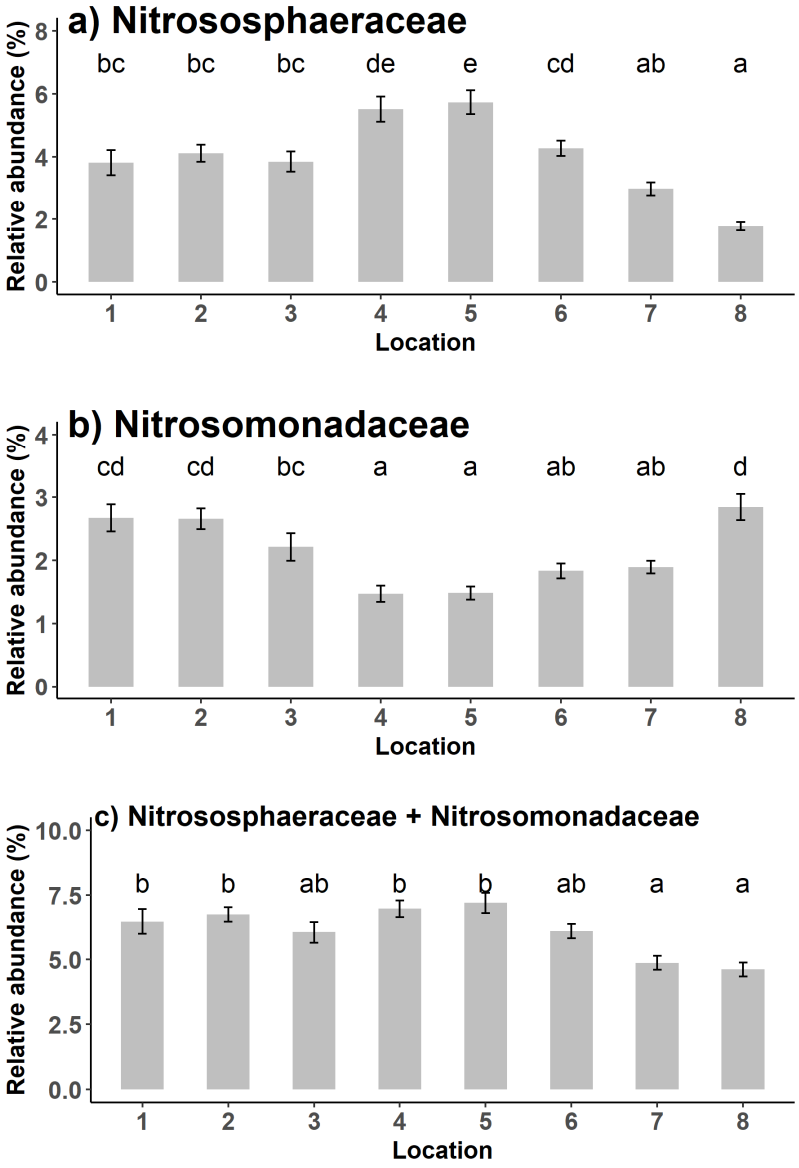

468

469 **Fig. 7**. Relative abundances of (a) *Nitrososphaeraceae*, (b) *Nitrosomonadaceae*, and (c) sum
470 of the two groups across topographic locations. Values are mean ± standard error (n = 11–12).
471 Letters not shared across locations represent significantly ($P < 0.01$) different means via
472 Tukey's multiple comparison test.

473

4. Discussion

In a humid corn-soybean rotation system, the dominant ecosystem type in the midwestern United States, we assessed variation in microbial community composition along a field-scale topographic gradient over time. We also investigated dominant drivers of this microbial variation and associations with measured biogeochemical processes. At a relatively high sampling frequency (approximately monthly), we found little change in microbial community composition over time despite large differences in weather and crop type (Fig. S1 and 2). Contrary to the small temporal variability, we found that microbial community composition varied greatly with topographic location and correlated strongly with soil moisture, SOC, and especially pH (Fig. 2 and 3). We found significant associations among a number of microbial groups (families and genera) and biogeochemical processes or pools, yet different ASVs within taxonomic groups often responded in opposite ways (Fig. 4 and 5; Table S3). Tradeoffs in specific ASVs among sampling locations (Fig. 6) likely contributed to relatively stable abundances in broader taxonomic groups across the gradient (Fig. S3), and tradeoffs in specific groups (Fig. 7) may explain similarities in rates of processes such as nitrification (Fig. 1).

4.1. Soil properties shaping microbial communities along the topographic gradient

Microbial community composition differed greatly across the topographic gradient and co-varied strongly with pH, SOC, and moisture (Fig. 2; Table S2). Soil pH related most strongly to bacterial composition (Table S2), consistent with previous findings at local and regional scales (Rousk et al., 2010; Griffiths et al., 2011). SOC and soil moisture are also well-known drivers of microbial community composition (Fierer et al., 2007; Maestre et al., 2015). The associations of these three factors with the microbiome were evident even at very broad (phylum and class) taxonomic levels (Fig. 3). Contrasting relationships between

relative abundances of *Acidobacteria* classes and pH, the relationships between *Actinobacteria* and pH, *Acidobacteria* and moisture, *Chloroflexi* and moisture, and *Verrucomicrobia* with all three variables are consistent with previous reports (Lauber et al., 2009; Maestre et al., 2015; Rousk et al., 2010; Zhang et al., 2020). However, SOC was positively related to oligotrophic *Chloroflexi* (Davis et al., 2011) and negatively related to copiotrophic *Bacteroidetes* (Fierer et al., 2007). These unexpected relationships may reflect that much of the SOC in the clay-rich depression soil, where SOC concentration was greatest, is not readily accessible to microbial decomposers due to protective associations with minerals (Li et al., 2018).

4.2. Associations among microbial groups and biogeochemical processes or pools

We also observed significant relationships among microbial groups and ASVs and dynamic biogeochemical variables (Fig. 4 and 5; Table S3). These findings are interesting as the capacity of microbial community composition to predict ecosystem functions remains under debate (E. K. Hall et al., 2018). For example, a significant correlation between *Nitrospira* abundance and N_2O emissions (Fig. 4) indicates a direct or indirect role of nitrification (or possibly comammox) as a control on N_2O in this humid ecosystem. *Nitrospira* typically mediates oxidation of nitrite to nitrate; it can also completely oxidize ammonia to nitrate in the comammox process (Daims et al., 2015). Therefore, its correlation with N_2O possibly reflects the importance of nitrate supply in controlling N_2O production via denitrification. Some probable denitrifiers, e.g., *Ferruginibacter*, *Litorilinea*, and *Cytophagaceae*, were positively correlated with ammonium ($NH_4^+{}_{initial}$) and/or nitrate ($NO_3^-{}_{initial}$) concentrations (Fig. 4), indicating that these organisms may reflect or respond to mineral N availability. Although specific mechanisms linking individual ASVs and environmental variables were not always clear (e.g., significant correlations of *Massilia* and *Phyllobacterium* with N_2O fluxes), our data illustrate the potential for 16S microbial

523 community composition data to provide an integrative measure of several ecosystem
524 functions.

525 We also found significant associations among HCl-extractable Fe pools and several
526 microbial groups and ASVs thought to participate in Fe reduction and oxidation (Fig. 5).
527 High concentrations of $Fe(II)_{HCl}$ indicate anoxic microsites where Fe reduction has occurred,
528 whereas high concentrations of $Fe(III)_{HCl}$ may indicate spatial or temporal redox gradients
529 where Fe(II) recently oxidized to form highly reactive Fe(III) phases. For example,
530 *Rhodomicrobium* was positively related to $Fe(II)_{HCl}$, consistent with its known metabolic role
531 as an Fe(II) oxidizer. $Fe(III)_{HCl}$ was positively correlated with Fe reducer *Bacillus* and
532 negatively correlated with Fe oxidizer *Thermomonas*, indicating their likely roles in driving
533 and responding to Fe redox cycling in this system. Our data are thus consistent with the
534 importance of oxygen availability and redox cycling in structuring the microbial communities
535 of these upland soils, a phenomenon that has received relatively little attention (Suriyavirun
536 et al., 2019; Yang and Liptzin, 2015). Furthermore, our data indicate that differences in
537 redox-sensitive Fe pools among sampling locations and time points are reflected in 16S
538 rRNA gene abundances of known Fe reducers and oxidizers.

539 We also observed significant relationships among biogeochemical variables (Table S3)
540 and ASVs corresponding to several globally dominant bacterial OTUs identified in a previous
541 synthesis (Delgado-Baquerizo et al., 2018), indicating that they may provide microbial
542 indicators of ecological functions or environmental conditions not only in this ecosystem but
543 possibly elsewhere. Several ASVs belonging to these globally dominant OTUs showed
544 relationships with $Fe(III)_{HCl}$ or $Fe(II)_{HCl}$, potentially indicating their sensitivity to soil O_2
545 availability even if they did not directly participate in Fe reduction or oxidation. Many ASVs
546 within the chitinolytic family *Chitinophagaceae* increased with $Fe(III)_{HCl}$, such as the
547 rarely-reported aerobic *Flavisolibacter* and *Segetibacter*. Similarly, *Haliangium*, known to

548 produce antifungal compounds, and rhizobacteria in the *Agromyces* genus showed positive
549 correlations with $Fe(III)_{HCl}$. A *Ferruginibacter* ASV within *Chitinophagaceae* was positively
550 related to both $Fe(III)_{HCl}$ and $NH_4^+{}_{initial}$. Combining microbial community composition data
551 with biogeochemical covariates provides a method for screening taxa for subsequent study as
552 potential microbial drivers of poorly understood biogeochemical processes. For example, in
553 Feammox, NH_4^+ oxidation is coupled to Fe(III) reduction, yet the microbial catalysts remain
554 poorly described (Yang et al., 2012). The roles of *Flavisolibacter*, *Pseudarthrobacter*, and
555 *WD2101_soil_group* in N-cycling also deserve further study given their relationships with
556 NH_4^+, NO_3^-, and/or N_2O flux. Although further evidence is needed for these findings,
557 significant relationships among microbial ASVs or groups and biogeochemical variables
558 indicate possible microbial linkages to particular ecosystem processes.

559 *4.3. Trade-offs among microbial groups and ASVs across topographic locations*

560 We found similar rates of several N-cycling processes across the topographic gradient
561 (Fig. 1; Table S1) despite large differences in moisture, pH, and total soil N, variables which
562 are known to influence N transformations in this ecosystem (S. J. Hall et al., 2018). This
563 finding might be partially explained by abundance trade-offs between different microbial
564 groups performing similar N-cycling functions. For example, both AOA (e.g.,
565 *Nitrososphaeraceae*) and AOB (e.g., *Nitrosomonadaceae*) are important ammonia oxidizers
566 in soil. Consistent with the commonly reported niche separation of ammonia oxidizers with
567 pH (Hu et al., 2014; Nicol et al., 2008), the relative abundances of these two groups showed
568 contrasting responses to location (Fig. 7a and 7b) and pH, suggesting that they segregated by
569 pH along the topographic gradient. Yet, their combined relative abundance remained
570 relatively consistent (Fig. 7c), possibly contributing to similar observed rates of net
571 nitrification across the gradient (Fig 1).

572 Notably, AOA had a strong positive relationship with pH while AOB had a negative

relationship with pH; AOA abundance and pH were highest in locations 4 and 5. Our findings agree with previous reports that AOA amoA gene abundance increased with pH (Gubry-Rangin et al., 2011; Hu et al., 2014). Opposite results have also been reported whereby AOA and AOB amoA gene abundances decreased and increased with pH, respectively (Fan et al., 2019; Nicol et al., 2008; Prosser and Nicol, 2012). These inconsistent findings suggest that soil niche specialization between AOA and AOB might also be affected by factors other than pH, e.g., availability of ammonium and organic carbon (Prosser and Nicol, 2012). We did not find significant correlations between AOA and AOB abundances and ammonium concentrations ($P > 0.50$). However, we found a positive relationship between AOA abundance and SOC ($r = 0.44$; $P < 0.05$) and no significant relationship between AOB abundance and SOC ($P > 0.05$), suggesting that greater C availability might have contributed to increased competitiveness of AOA over AOB at locations 4 and 5 if some of these organisms were heterotrophic or mixotrophic (Prosser and Nicol, 2012).

We also observed abundance trade-offs among ASVs within particular phyla across topographic locations (Fig. 6) even while overall phyla abundances remained similar across the gradient (Fig. S3). Other studies have also reported similar phyla abundances across topographic gradients within a site (Schlatter et al., 2019; Suriyavirun et al., 2019), but here, we found strong shifts in individual ASVs among sampling locations that were masked by general similarities at the phylum level (Fig. S3). Furthermore, ASVs nested within broader taxonomic groups often correlated in opposite ways with biogeochemical variables (Fig. 4 and 5), challenging the idea that ASVs from the same OTUs are functionally equivalent (García-García et al., 2019). These results suggest that closely related taxa may respond differently to environmental variation (Bier et al., 2015). This conclusion is supported by observations of distinct genomic contents and unique features among subpopulations of the same species in two genomic studies (Kashtan et al., 2014; Rasko et al., 2008). Taken

598 together, our observational results are consistent with the hypothesis that individuals from the
599 same families or genera are not necessarily functionally or ecologically coherent.

600 *4.4. Little change in community composition over time*

601 Few studies have assessed inter-annual variations in agricultural soil microbial
602 communities on a monthly basis (Hsiao et al., 2019). With this relatively high temporal
603 sampling frequency, we found that microbial evenness (inverse Simpson index) was
604 significantly higher at the peak and the end of the growing season (July to October) than in
605 the early-growing season (March to June); microbial richness (Chao1 index) showed a similar
606 but insignificant trend (Fig. S2). Bacterial richness and diversity were also higher in the
607 peak-growing season (August) than in the early-growing season (late May to early June) in
608 prairie and continuous corn soils located several km from our site (Upton et al., 2019),
609 possibly driven by greater litter inputs and exudates during this period (Lauber et al., 2013).

610 Different from microbial evenness, microbial community composition changed little
611 over time within and among years, despite large variation in weather and crop type (Fig. S1).
612 Moderate (Bainard et al., 2016; Hsiao et al., 2019; Lauber et al., 2013) or minor (Bainard et
613 al., 2016; Smith et al., 2016; Yu et al., 2011) temporal changes in microbial community
614 composition have been reported for agricultural soils. Three reasons might explain why
615 sampling month and year had minor effects on microbial community composition in our
616 study. First, SOC contents were high in these soils relative to many other agroecosystems
617 (Bainard et al., 2016; Lauber et al., 2013), and stable isotopes indicated that C derived from
618 the most recent crop residues accounted for a small fraction of total soil respiration in nearby
619 soils under similar management (Ye and Hall, 2020). Therefore, these communities may be
620 more temporally stable because most soil metabolic activity is focused on processing
621 slower-cycling C pools (with turnover times of years to decades) as opposed to the most
622 recent litter inputs. Second, a large pool of relic DNA persisting in soil for weeks to years

after cell death may buffer temporal changes, a phenomenon that may be especially pronounced in neutral and alkaline soils such as those examined here (Carini et al., 2016). Third, strong spatial variability in soil properties such as pH are strong determinants of bacterial community composition (Fig. 1 and Table S2) and may mask temporal/crop variability across broad gradients in soil properties (Bainard et al., 2016; De Gruyter et al., 2020; Fierer and Jackson, 2006). Overall, community composition was quite constant over time, despite the fact that some individual taxonomic groups and ASVs correlated with spatiotemporal variation in biogeochemical processes.

5. Conclusion

Here, we found that microbial community composition varied greatly with topographic location but changed little among months and years despite large differences in weather and crop type in a corn-soybean rotation. Tradeoffs in specific ASVs or groups such as AOA vs AOB among topographic locations may explain relatively similar abundances of dominant taxonomic groups and process rates such as nitrification. We found significant associations among many microbial groups and ASVs with metrics of N, Fe, and C cycling, which varied more over time than over space. Notably, different ASVs within the same families or genera often had opposite relationships with biogeochemical variables, challenging previous statements that closely related taxa are functionally redundant. Our results indicate that spatial and temporal variation in microbial composition among samples can potentially provide insights into ecosystem processes.

Acknowledgements

This research was supported in part by USDA-AFRI award 2018-67019-27886 and the Iowa Nutrient Research Center.

References

Bainard, L.D., Hamel, C., Gan, Y., 2016. Edaphic properties override the influence of crops on the composition of the soil bacterial community in a semiarid agroecosystem. Applied Soil Ecology 105, 160–168. doi:10.1016/j.apsoil.2016.03.013

Bates, D., Maechler, M., Bolker, B., Walker, S., 2015. Fitting linear mixed-effects models using lme4. Journal of Statistical Software 67, 1–48. doi:10.18637/jss.v067.i01

Bier, R.L., Voss, K.A., Bernhardt, E.S., 2015. Bacterial community responses to a gradient of alkaline mountaintop mine drainage in Central Appalachian streams. The ISME Journal 9, 1378–1390. doi:10.1038/ismej.2014.222

Butterbach-Bahl, K., Baggs, E.M., Dannenmann, M., Kiese, R., Zechmeister-Boltenstern, S., 2013. Nitrous oxide emissions from soils: how well do we understand the processes and their controls? Philosophical Transactions: Biological Sciences 368, 1–13. doi:10.1098/rstb.2013.0122

Callahan, B.J., McMurdie, P.J., Rosen, M.J., Han, A.W., Johnson, A.J.A., Holmes, S.P., 2016. DADA2: High-resolution sample inference from Illumina amplicon data. Nature Methods 13, 581–583. doi:10.1038/nmeth.3869

Cao, P., Lu, C., Yu, Z., 2018. Historical nitrogen fertilizer use in agricultural ecosystems of the contiguous United States during 1850–2015: application rate, timing, and fertilizer types. Earth System Science Data 10, 969–984. doi:10.5194/essd-10-969-2018

Caporaso, J.G., 2018. EMP 16S Illumina Amplicon Protocol.

Carini, P., Marsden, P.J., Leff, J.W., Morgan, E.E., Strickland, M.S., Fierer, N., 2016. Relic DNA is abundant in soil and obscures estimates of soil microbial diversity. Nature Microbiology 2, 1–6. doi:10.1038/nmicrobiol.2016.242

Daims, H., Lebedeva, E.V., Pjevac, P., Han, P., Herbold, C., Albertsen, M., Jehmlich, N.,

Palatinszky, M., Vierheilig, J., Bulaev, A., Kirkegaard, R.H., von Bergen, M., Rattei, T., Bendinger, B., Nielsen, P.H., Wagner, M., 2015. Complete nitrification by *Nitrospira* bacteria. Nature 528, 504–509. doi:10.1038/nature16461

Davis, K.E.R., Sangwan, P., Janssen, P.H., 2011. *Acidobacteria, Rubrobacteridae* and *Chloroflexi* are abundant among very slow-growing and mini-colony-forming soil bacteria. Environmental Microbiology 13, 798–805. doi:10.1111/j.1462-2920.2010.02384.x

De Gruyter, J., Weedon, J.T., Bazot, S., Dauwe, S., Fernandez-Garberí, P.-R., Geisen, S., De La Motte, L.G., Heinesch, B., Janssens, I.A., Leblans, N., Manise, T., Ogaya, R., Löfvenius, M.O., Peñuelas, J., Sigurdsson, B.D., Vincent, G., Verbruggen, E., 2020. Patterns of local, intercontinental and interseasonal variation of soil bacterial and eukaryotic microbial communities. FEMS Microbiology Ecology 96, fiaa018. doi:10.1093/femsec/fiaa018

Delgado-Baquerizo, M., Oliverio, A.M., Brewer, T.E., Benavent-González, A., Eldridge, D.J., Bardgett, R.D., Maestre, F.T., Singh, B.K., Fierer, N., 2018. A global atlas of the dominant bacteria found in soil. Science 359, 320–325. doi:10.1126/science.aap9516

Doane, T.A., Horwáth, W.R., 2003. Spectrophotometric determination of nitrate with a single reagent. Analytical Letters 36, 2713–2722. doi:10.1081/AL-120024647

Domeignoz□Horta, L.A., Philippot, L., Peyrard, C., Bru, D., Breuil, M.-C., Bizouard, F., Justes, E., Mary, B., Léonard, J., Spor, A., 2018. Peaks of in situ N_2O emissions are influenced by N_2O-producing and reducing microbial communities across arable soils. Global Change Biology 24, 360–370. doi:10.1111/gcb.13853

Esther, J., Sukla, L.B., Pradhan, N., Panda, S., 2015. Fe (III) reduction strategies of dissimilatory iron reducing bacteria. Korean Journal of Chemical Engineering 32, 1–14. doi:10.1007/s11814-014-0286-x

695 Fan, X., Yin, C., Chen, H., Ye, M., Zhao, Y., Li, T., Wakelin, S.A., Liang, Y., 2019. The
696 efficacy of 3,4-dimethylpyrazole phosphate on N_2O emissions is linked to niche
697 differentiation of ammonia oxidizing archaea and bacteria across four arable soils.
698 Soil Biology and Biochemistry 130, 82–93. doi:10.1016/j.soilbio.2018.11.027
699 Fierer, N., Bradford, M.A., Jackson, R.B., 2007. Toward an ecological classification of soil
700 bacteria. Ecology 88, 1354–1364. doi:10.1890/05-1839
701 Fierer, N., Jackson, R.B., 2006. The diversity and biogeography of soil bacterial
702 communities. Proceedings of the National Academy of Sciences of the United States
703 of America 103, 626–631. doi:10.1073/pnas.0507535103
704 García-García, N., Tamames, J., Linz, A.M., Pedrós-Alió, C., Puente-Sánchez, F., 2019.
705 Microdiversity ensures the maintenance of functional microbial communities under
706 changing environmental conditions. The ISME Journal 13, 2969–2983.
707 doi:10.1038/s41396-019-0487-8
708 Gelder, B.K., 2015. Automation of DEM cutting for hydrologic/hydraulic modeling.
709 Technical Report to the Iowa State University. Institute for Transportation, Ames,
710 Iowa.
711 Griffis, T.J., Chen, Z., Baker, J.M., Wood, J.D., Millet, D.B., Lee, X., Venterea, R.T., Turner,
712 P.A., 2017. Nitrous oxide emissions are enhanced in a warmer and wetter world.
713 Proceedings of the National Academy of Sciences 114, 12081–12085.
714 doi:10.1073/pnas.1704552114
715 Griffiths, R.I., Thomson, B.C., James, P., Bell, T., Bailey, M., Whiteley, A.S., 2011. The
716 bacterial biogeography of British soils. Environmental Microbiology 13, 1642–1654.
717 doi:10.1111/j.1462-2920.2011.02480.x
718 Gubry-Rangin, C., Hai, B., Quince, C., Engel, M., Thomson, B.C., James, P., Schloter, M.,
719 Griffiths, R.I., Prosser, J.I., Nicol, G.W., 2011. Niche specialization of terrestrial

archaeal ammonia oxidizers. Proceedings of the National Academy of Sciences 108, 21206–21211. doi:10.1073/pnas.1109000108

Guo, J., Cong, Q., Zhang, L., Meng, L., Ma, F., Zhang, J., 2019. Exploring the linkage between bacterial community composition and nitrous oxide emission under varied DO levels through the alternation of aeration rates in a lab-scale anoxic-oxic reactor. Bioresource Technology 291, 121809. doi:10.1016/j.biortech.2019.121809

Hall, E.K., Bernhardt, E.S., Bier, R.L., Bradford, M.A., Boot, C.M., Cotner, J.B., Del Giorgio, P.A., Evans, S.E., Graham, E.B., Jones, S.E., Lennon, J.T., Locey, K.J., Nemergut, D., Osborne, B.B., Rocca, J.D., Schimel, J.P., Waldrop, M.P., Wallenstein, M.D., 2018. Understanding how microbiomes influence the systems they inhabit. Nature Microbiology 3, 977–982. doi:10.1038/s41564-018-0201-z

Hall, S.J., McDowell, W.H., Silver, W.L., 2013. When wet gets wetter: Decoupling of moisture, redox biogeochemistry, and greenhouse gas fluxes in a humid tropical forest soil. Ecosystems 16, 576–589. doi:10.1007/s10021-012-9631-2

Hall, S.J., Reyes, L., Huang, W., Homyak, P.M., 2018. Wet spots as hotspots: Moisture responses of nitric and nitrous oxide emissions from poorly drained agricultural soils. Journal of Geophysical Research: Biogeosciences 123, 3589–3602. doi:10.1029/2018JG004629

Hsiao, C.-J., Sassenrath, G.F., Zeglin, L.H., Hettiarachchi, G.M., Rice, C.W., 2019. Temporal variation of soil microbial properties in a corn–wheat–soybean system. Soil Science Society of America Journal 83, 1696–1711. doi:10.2136/sssaj2019.05.0160

Hu, B., Liu, S., Wang, W., Shen, L., Lou, L., Liu, W., Tian, G., Xu, X., Zheng, P., 2014. pH-dominated niche segregation of ammonia-oxidising microorganisms in Chinese agricultural soils. FEMS Microbiology Ecology 90, 290–299. doi:10.1111/1574-6941.12391

745 Hu, H.-W., Chen, D., He, J.-Z., 2015. Microbial regulation of terrestrial nitrous oxide
746 formation: understanding the biological pathways for prediction of emission rates.
747 FEMS Microbiology Reviews 39, 729–749. doi:10.1093/femsre/fuv021
748 Huang, W., Hall, S.J., 2017a. Elevated moisture stimulates carbon loss from mineral soils by
749 releasing protected organic matter. Nature Communications 8, 1–10.
750 doi:10.1038/s41467-017-01998-z
751 Huang, W., Hall, S.J., 2017b. Optimized high-throughput methods for quantifying iron
752 biogeochemical dynamics in soil. Geoderma 306, 67–72.
753 doi:10.1016/j.geoderma.2017.07.013
754 Jafari, M., Ansari-Pour, N., 2019. Why, when and how to adjust your P values? Cell Journal
755 20, 604–607. doi:10.22074/cellj.2019.5992
756 Jones, C.S., Nielsen, J.K., Schilling, K.E., Weber, L.J., 2018. Iowa stream nitrate and the
757 Gulf of Mexico. PLOS ONE 13, e0195930. doi:10.1371/journal.pone.0195930
758 Kashtan, N., Roggensack, S.E., Rodrigue, S., Thompson, J.W., Biller, S.J., Coe, A., Ding, H.,
759 Marttinen, P., Malmstrom, R.R., Stocker, R., Follows, M.J., Stepanauskas, R.,
760 Chisholm, S.W., 2014. Single-cell genomics reveals hundreds of coexisting
761 subpopulations in wild *Prochlorococcus*. Science 344, 416–420.
762 doi:10.1126/science.1248575
763 Kuypers, M.M.M., Marchant, H.K., Kartal, B., 2018. The microbial nitrogen-cycling
764 network. Nature Reviews Microbiology 16, 263–276. doi:10.1038/nrmicro.2018.9
765 Lauber, C.L., Hamady, M., Knight, R., Fierer, N., 2009. Pyrosequencing-based assessment of
766 soil pH as a predictor of soil bacterial community structure at the continental scale.
767 Applied and Environmental Microbiology 75, 5111–5120.
768 doi:10.1128/AEM.00335-09

769 Lauber, C.L., Ramirez, K.S., Aanderud, Z., Lennon, J., Fierer, N., 2013. Temporal variability
770 in soil microbial communities across land-use types. The ISME Journal 7, 1641–1650.
771 doi:10.1038/ismej.2013.50
772 Lawrence, N.C., Hall, S.J., 2020. Capturing temporal heterogeneity in soil nitrous oxide
773 fluxes with a robust and low-cost automated chamber apparatus. Atmospheric
774 Measurement Techniques 13, 4065–4078. doi:10.5194/amt-13-4065-2020
775 Li, X., McCarty, G.W., Karlen, D.L., Cambardella, C.A., Effland, W., 2018. Soil organic
776 carbon and isotope composition response to topography and erosion in Iowa. Journal
777 of Geophysical Research: Biogeosciences 123, 3649–3667.
778 doi:10.1029/2018JG004824
779 Logsdon, S.D., James, D.E., 2014. Closed depression topography Harps soil, revisited. Soil
780 Horizons 55, sh13-11–0025. doi:10.2136/sh13-11-0025
781 Love, M.I., Huber, W., Anders, S., 2014. Moderated estimation of fold change and dispersion
782 for RNA-seq data with DESeq2. Genome Biology 15, 550.
783 doi:10.1186/s13059-014-0550-8
784 Maestre, F.T., Delgado-Baquerizo, M., Jeffries, T.C., Eldridge, D.J., Ochoa, V., Gozalo, B.,
785 Quero, J.L., García-Gómez, M., Gallardo, A., Ulrich, W., Bowker, M.A., Arredondo,
786 T., Barraza-Zepeda, C., Bran, D., Florentino, A., Gaitán, J., Gutiérrez, J.R.,
787 Huber-Sannwald, E., Jankju, M., Mau, R.L., Miriti, M., Naseri, K., Ospina, A., Stavi,
788 I., Wang, D., Woods, N.N., Yuan, X., Zaady, E., Singh, B.K., 2015. Increasing aridity
789 reduces soil microbial diversity and abundance in global drylands. Proceedings of the
790 National Academy of Sciences 112, 15684–15689. doi:10.1073/pnas.1516684112
791 Martin, A.R., Kaleita, A.L., Soupir, M.L., 2019. Inundation patterns of farmed pothole
792 depressions with varying subsurface drainage. Transactions of the ASABE 62, 1579–
793 1590. doi:10.13031/trans.13435

McMurdie, P.J., Holmes, S., 2013. phyloseq: An R package for reproducible interactive analysis and graphics of microbiome census data. PLOS ONE 8, e61217. doi:10.1371/journal.pone.0061217

Nicol, G.W., Leininger, S., Schleper, C., Prosser, J.I., 2008. The influence of soil pH on the diversity, abundance and transcriptional activity of ammonia oxidizing archaea and bacteria. Environmental Microbiology 10, 2966–2978. doi:10.1111/j.1462-2920.2008.01701.x

Oksanen, J., Blanchet, F.G., Friendly, M., Kindt, R., Legendre, P., McGlinn, D., Minchin, P.R., O'Hara, R.B., Simpson, G.L., Solymos, P., Stevens, M.H.H., Szoecs, E., Wagner, H., 2019. Vegan: community ecology package. R package version 2.5-4.

Ouyang, Y., Norton, J.M., 2020. Nitrite oxidizer activity and community are more responsive than their abundance to ammonium-based fertilizer in an agricultural soil. Frontiers in Microbiology 11, Article 1736. doi:10.3389/fmicb.2020.01736

Petersen, D.G., Blazewicz, S.J., Firestone, M., Herman, D.J., Turetsky, M., Waldrop, M., 2012. Abundance of microbial genes associated with nitrogen cycling as indices of biogeochemical process rates across a vegetation gradient in Alaska. Environmental Microbiology 14, 993–1008. doi:10.1111/j.1462-2920.2011.02679.x

Pett-Ridge, J., Firestone, M.K., 2005. Redox fluctuation structures microbial communities in a wet tropical soil. Applied and Environmental Microbiology 71, 6998–7007. doi:10.1128/AEM.71.11.6998-7007.2005

Philippot, L., Andersson, S.G.E., Battin, T.J., Prosser, J.I., Schimel, J.P., Whitman, W.B., Hallin, S., 2010. The ecological coherence of high bacterial taxonomic ranks. Nature Reviews Microbiology 8, 523–529. doi:10.1038/nrmicro2367

817 Philippot, L., Germon, J.C., 2005. Chapter eight - Contribution of bacteria to initial input and
818 cycling of nitrogen in soils, in: Buscot, F., Varma, A. (Eds.), Microorganisms in Soils:
819 Roles in Genesis and Functions. Springer, Berlin, Heidelberg, pp. 159–176.
820 Pitombo, L.M., Carmo, J.B. do, Hollander, M. de, Rossetto, R., López, M.V., Cantarella, H.,
821 Kuramae, E.E., 2016. Exploring soil microbial 16S rRNA sequence data to increase
822 carbon yield and nitrogen efficiency of a bioenergy crop. GCB Bioenergy 8, 867–879.
823 doi:10.1111/gcbb.12284
824 Prosser, J.I., 2015. Dispersing misconceptions and identifying opportunities for the use of
825 “omics” in soil microbial ecology. Nature Reviews Microbiology 13, 439–446.
826 doi:10.1038/nrmicro3468
827 Prosser, J.I., Nicol, G.W., 2012. Archaeal and bacterial ammonia oxidisers in soil: the quest
828 for niche specialisation and differentiation. Trends in Microbiology 20, 523–531.
829 doi:10.1016/j.tim.2012.08.001
830 R Core Team, 2019. R: A language and environment for statistical computing. R Foundation
831 for Statistical Computing, Vienna, Austria.
832 Ramírez-Flandes, S., González, B., Ulloa, O., 2019. Redox traits characterize the
833 organization of global microbial communities. Proceedings of the National Academy
834 of Sciences 116, 3630–3635. doi:10.1073/pnas.1817554116
835 Rasko, D.A., Rosovitz, M.J., Myers, G.S.A., Mongodin, E.F., Fricke, W.F., Gajer, P.,
836 Crabtree, J., Sebaihia, M., Thomson, N.R., Chaudhuri, R., Henderson, I.R., Sperandio,
837 V., Ravel, J., 2008. The pangenome structure of *Escherichia coli*: Comparative
838 genomic analysis of *E. coli* commensal and pathogenic isolates. Journal of
839 Bacteriology 190, 6881–6893. doi:10.1128/JB.00619-08

Rousk, J., Bååth, E., Brookes, P.C., Lauber, C.L., Lozupone, C., Caporaso, J.G., Knight, R., Fierer, N., 2010. Soil bacterial and fungal communities across a pH gradient in an arable soil. The ISME Journal 4, 1340–1351. doi:10.1038/ismej.2010.58

Schlatter, D.C., Reardon, C.L., Johnson-Maynard, J., Brooks, E., Kahl, K., Norby, J., Huggins, D., Paulitz, T.C., 2019. Mining the drilosphere: Bacterial communities and denitrifier abundance in a no-till wheat cropping system. Frontiers in Microbiology 10, Article 1339. doi:10.3389/fmicb.2019.01339

Smith, C.R., Blair, P.L., Boyd, C., Cody, B., Hazel, A., Hedrick, A., Kathuria, H., Khurana, P., Kramer, B., Muterspaw, K., Peck, C., Sells, E., Skinner, J., Tegeler, C., Wolfe, Z., 2016. Microbial community responses to soil tillage and crop rotation in a corn/soybean agroecosystem. Ecology and Evolution 6, 8075–8084. doi:10.1002/ece3.2553

Smith, S., 2019. phylosmith: an R-package for reproducible and efficient microbiome analysis with phyloseq-objects. Journal of Open Source Software 4, 1442. doi:10.21105/joss.01442

Spohn, M., Klaus, K., Wanek, W., Richter, A., 2016. Microbial carbon use efficiency and biomass turnover times depending on soil depth – Implications for carbon cycling. Soil Biology and Biochemistry 96, 74–81. doi:10.1016/j.soilbio.2016.01.016

Suriyavirun, N., Krichels, A.H., Kent, A.D., Yang, W.H., 2019. Microtopographic differences in soil properties and microbial community composition at the field scale. Soil Biology and Biochemistry 131, 71–80. doi:10.1016/j.soilbio.2018.12.024

Upton, R.N., Bach, E.M., Hofmockel, K.S., 2019. Spatio-temporal microbial community dynamics within soil aggregates. Soil Biology and Biochemistry 132, 58–68. doi:10.1016/j.soilbio.2019.01.016

Weatherburn, M.W., 1967. Phenol-hypochlorite reaction for determination of ammonia. Analytical Chemistry 39, 971–974. doi:10.1021/ac60252a045

Weber, K.A., Achenbach, L.A., Coates, J.D., 2006. Microorganisms pumping iron: anaerobic microbial iron oxidation and reduction. Nature Reviews Microbiology 4, 752–764. doi:10.1038/nrmicro1490

Yang, W.H., Liptzin, D., 2015. High potential for iron reduction in upland soils. Ecology 96, 2015–2020. doi:10.1890/14-2097.1

Yang, W.H., Weber, K.A., Silver, W.L., 2012. Nitrogen loss from soil through anaerobic ammonium oxidation coupled to iron reduction. Nature Geoscience 5, 538–541. doi:10.1038/ngeo1530

Ye, C., Hall, S.J., 2020. Mechanisms underlying limited soil carbon gains in perennial and cover-cropped bioenergy systems revealed by stable isotopes. GCB Bioenergy 12, 101–117. doi:10.1111/gcbb.12657

Yu, Z., Wang, G., Jin, J., Liu, J., Liu, X., 2011. Soil microbial communities are affected more by land use than seasonal variation in restored grassland and cultivated Mollisols in Northeast China. European Journal of Soil Biology 47, 357–363. doi:10.1016/j.ejsobi.2011.09.001

Zhang, X., Gao, G., Wu, Z., Wen, X., Zhong, H., Zhong, Z., Yang, C., Bian, F., Gai, X., 2020. Responses of soil nutrients and microbial communities to intercropping medicinal plants in moso bamboo plantations in subtropical China. Environmental Science and Pollution Research 27, 2301–2310. doi:10.1007/s11356-019-06750-2

- Several microbial groups correlated significantly with N- or Fe-cycling processes
- Different taxa within the same phylogenetic groups often responded in opposite ways
- Microbial composition varied with topographic location but changed little over time
- Ammonia-oxidizing archaea and bacteria varied inversely but their sum was similar
- Composition tradeoffs might maintain similar process rates across soil gradients

Declaration of interests

☒ The authors declare that they have no known competing financial interests or personal relationships that could have appeared to influence the work reported in this paper.

☐The authors declare the following financial interests/personal relationships which may be considered as potential competing interests: